Magnetotelluric measurements across the Beattie magnetic anomaly and the Southern Cape Conductive Belt, South Africa

U. Weckmann,[1,2] O. Ritter,[2] A. Jung,[2] T. Branch,[2,3] and M. de Wit[3]

Received 3 August 2005; revised 21 June 2006; accepted 28 November 2006; published 25 May 2007.

[1] The Beattie Magnetic Anomaly (BMA) and the Southern Cape Conductive Belt (SCCB), two of Earth's largest continental geophysical anomalies, extend across the southern African continent in an east-west direction. To resolve structural details of the SCCB, a high-resolution magnetotelluric study was conducted in March 2004, along a 150-km-long N-S profile across the Karoo Basin in South Africa. A two-dimensional conductivity model at a scale of the entire crust exhibits three distinct zones of high conductivity: (1) Beneath the surface trace of the axis of the BMA we observe a high-conductivity anomaly at 5 to 10 km depth; however, it remains enigmatic whether both geophysical anomalies have the same source. (2) A shallow, regionally continuous subhorizontal band of high conductivity can be linked to a 50- to 70-m-thick pyritic-carbonaceous marker horizon intersected in deep boreholes. (3) Several highly conductive synformal features in the mid crust are newly imaged near the northern extremity of the profile. Our data generally support the existence of a deeper conductivity belt but allow for a much better definition of crustal conductivity in this region. Such laterally confined zones of crustal conductivity can only be resolved with a dense site spacing and broadband recordings.

Citation: Weckmann, U., O. Ritter, A. Jung, T. Branch, and M. de Wit (2007), Magnetotelluric measurements across the Beattie magnetic anomaly and the Southern Cape Conductive Belt, South Africa, *J. Geophys. Res.*, *112*, B05416, doi:10.1029/2005JB003975.

1. Introduction

[2] South Africa hosts two of Earth's largest known continental geophysical anomalies, the Beattie Magnetic Anomaly (BMA) and the near coincident Southern Cape Conductive Belt (SCCB), both of which extend across South Africa for almost 1000 km in an east-west direction (see Figure 1). These anomalies likely continued even farther, into Antarctica and southern South America, before they were truncated in the Cretaceous by the Agulhas Fracture Zone in the east and the margins of the South Atlantic in the west, following the breakout of southern Africa from Gondwana [*de Beer et al.*, 1982; *Corner*, 1989].

[3] The BMA was discovered by *Beattie* [1909] early last century as a large positive static magnetic anomaly. Modeling by *Pitts et al.* [1992] suggests that an approximately 30 km broad magnetic body, dipping south from 7 km below surface to a depth of ~30 km, is required to explain this magnetic anomaly. A similar depth to the top of the anomaly (~8 km) was inferred from seismic receiver function analysis [*Harvey et al.*, 2001]. This latter analysis also indicates a slight deepening of the anomaly to 11 km at the western extremity of the BMA.

[4] Magnetometer array studies in the 1970s led to the discovery of a ~140-km-wide high electrically conductive structure in the crystalline crust or upper mantle. This conductive anomaly was named the Southern Cape Conductive Belt [*Gough et al.*, 1973; *de Beer et al.*, 1982]. In our study area (~21°E), the southern boundary of the SCCB extends for about 40 km beneath the mountainous terrain of the Cape Fold Belt (CFB) while its northern boundary in this area, when projected to surface, is nearly coincident with the Great Escarpment [cf. *King*, 1963] (Figure 2a), but which the SCCB transgresses on a regional scale. The SCCB so far has only been detected by means of geomagnetic depth soundings (GDS) and is restricted to a period range of 1000–12,000 s [*de Beer and Gough*, 1980]. This seems to correspond with a lower crustal or upper mantle depth; however, GDS is ambiguous with respect to depth resolution.

[5] Because of the spatial coincidence between the BMA and the northern edge of the SCCB, a common source is generally assumed. A segment of partially serpentinized paleo-oceanic lithosphere embedded in crystalline basement was considered as the most likely explanation for the anomalies by *de Beer et al.* [1982]. This basement, however, is not

[1]Dublin Institute for Advanced Studies, School of Cosmic Physics, Dublin, Ireland.
[2]GeoForschungsZentrum Potsdam, Potsdam, Germany.
[3]Centre for Interactive Graphical Computing of Earth Systems, Department of Geological Sciences, University of Cape Town, Rondebosch, Republic of South Africa.

0148-0227/07/2005JB003975$09.00

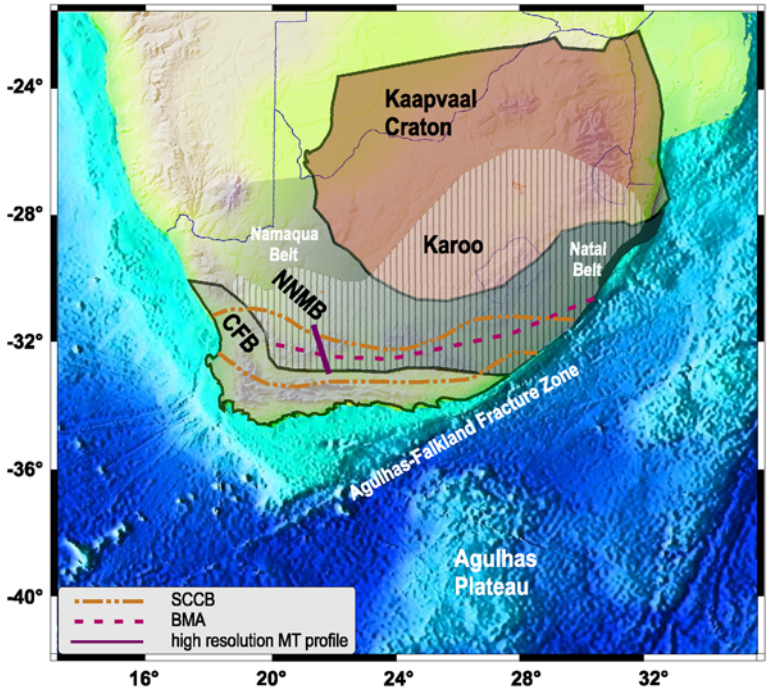

Figure 1. Simplified tectonic map of southern Africa showing the Archean Kaapvaal Craton, the Mesoproterozoic Namaqua Natal Mobile Belt (NNMB), and the upper Paleozoic Cape Fold Belt (CFB). A vast area is covered by Paleozoic-Mesozoic sediments and igneous rocks of the Karoo Basin. The axis of the Beattie Magnetic Anomaly (BMA, dashed line) and the boundaries of the Southern Cape Conductive Belt (SCCB, dot-dashed line [cf. *de Beer et al.*, 1982, Figure 12]) are marked. The location of the MT profile is shown by a black line.

exposed at surface in the area of interest north of the CFB. Nevertheless, the high-grade Mesoproterozoic granitoid basement (1.0–2.0 Ga) to the north of the BMA (as determined through drilling) is different from the low-grade Neoproterozoic metasediments (0.5–0.6 Ga) exposed south of the CFB thrust front (see Figure 1). Other workers have suggested therefore that the inferred serpentinites might represent a suture zone defining the southern margin of this Mesoproterozoic basement, known as the Natal-Namaqua Mobile Belt (NNMB) [*Pitts et al.*, 1992; *Harvey et al.*, 2001]. In contrast, *Corner* [1989] inferred that mineralized thrust zones within the NNMB granitoid basement were a more likely explanation for the anomalies. Alternatively, shear zones bounding elongated granitoid terranes that constitute the NNMB in Natal, along the coast of the Indian Ocean, are inferred as the most likely cause for the BMA by *Thomas et al.* [1992] from their integrated studies along the Natal coast of the Indian Ocean.

[6] Drilling has shown that the crystalline basement in the study area is overlain by a ~6-km-thick sequence of sediments of the Paleozoic-Mesozoic Cape and Karoo basins [*Söhnge and Hälbich*, 1983] (see also Figure 1). Projected to surface, the BMA anomaly occurs roughly 50 km north of the exposed thrust front of the Cape Fold Belt (CFB) in the west of the country (e.g., close to Prince Albert in the present study area). Toward the east, beyond ~24°E, the BMA and CFB front diverge sharply, with the BMA (and the SCCB) striking northeast, parallel to the structural grain of the NNMB, while the CFB structures deflect toward the southeast (see Figure 1). Thus, while the anomalies are apparently confined to the NNMB, the origin of the anomalies remains unknown.

[7] In this study we report on modern high-resolution magnetotelluric measurements across the anomalies. The magnetotelluric (MT) method in general is superior to the GDS with respect to depth resolution. The data presented here were acquired within the framework of the German-South African Inkaba yeAfrica project [*Bochannon*, 2004; *de Wit and Horsfield*, 2006], in which the MT profile is part of a much longer onshore/offshore geotraverse from the Agulhas plateau into the Karoo including ongoing magnetotelluric (MT), seismic and geological investigations.

2. Geological Setting

[8] The landscape of the study area is characterized by two regional terrains separated by a steeply dipping erosional scarp known as the Great Escarpment (see northern black dashed line in Figure 2a). Although the precise origin of the Great Escarpment is still under dispute, recent fission track analyses indicate that the scarp formed near its present location shortly after the break up of Gondwana (J. Tinker et al., Quantifying South African Uplift: Using apatite fission track thermochronology and offshore sediment volumes to test the balance between onshore denudation and offshore accumulation since Gondwana break-up, manuscript in preparation, 2005). North of the Great Escarpment, thick dolerite sills and dikes of Jurassic age (~182 Ma) are common and control the geomorphic evolution of the landscape [*King*, 1963]; south of the Great Escarpment dolerite

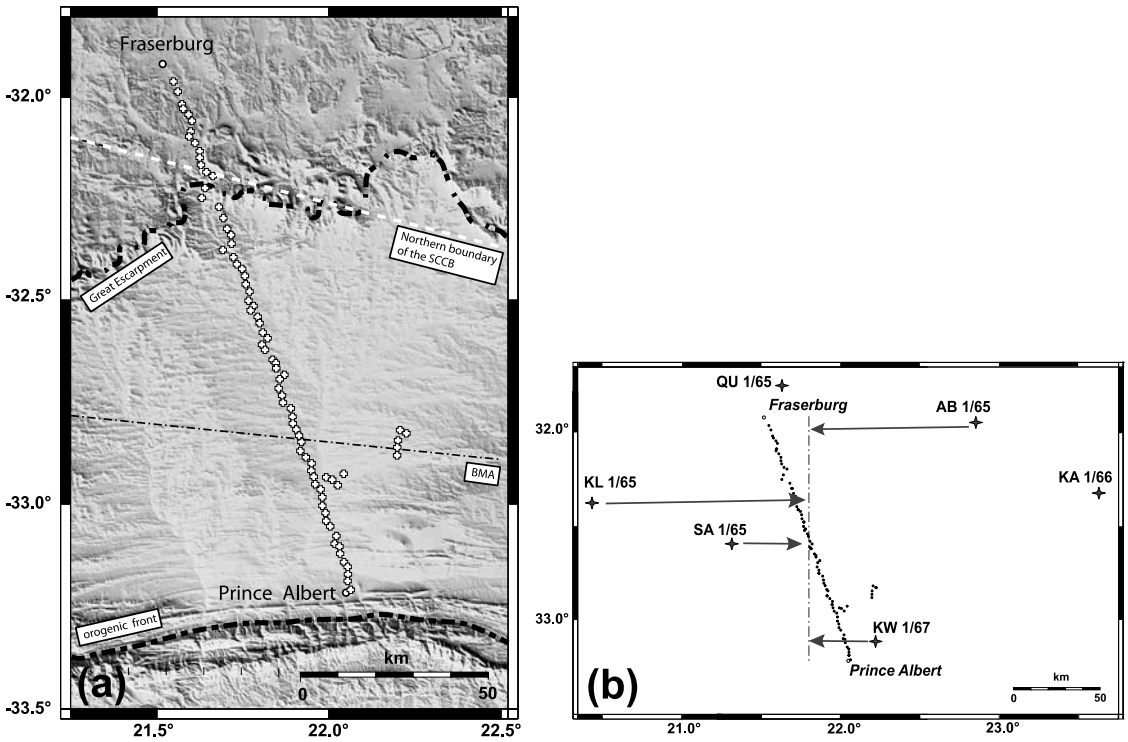

Figure 2. (a) Location of 82 MT sites deployed along a 150 km long profile from Prince Albert to Fraserburg. Nine additional sites near the surface trace of the BMA (Beattie Magnetic Anomaly) were located to the east of the main profile where it crosses the DC railway system to ensure good data quality in this part of the profile. The black dashed line in the north delineates the location of the Great Escarpment. To the south of Prince Albert the black dashed line marks the orogenic front of the CFB. (b) Location of the MT sites and the profile used for the two-dimensional inversion studies (gray dot-dashed line) together with selected deep boreholes (stars) and their projection (arrows) onto the profile. For the projection we used the strike direction of the Karoo Basin which is in east-west direction.

intrusions are scarce and are seldom intersected in the numerous boreholes. The landscape along our profile is relatively flat south of the Great Escarpment until it reaches the foothills (and thrust front) of the Cape Fold Belt (CFB) close to Prince Albert at the southern end of the profile (see southern black dashed line in Figure 2a). The entire area of interest is underlain by Paleozoic sediments of the Cape and Karoo basins; Mesozoic parts of the Karoo Basin occur only to the north of the study area.

[9] The main Karoo Basin has been modeled as a foreland basin formed in response to the formation of the CFB to the south [*Cole*, 1992; *Cloetingh et al.*, 1992; *Johnson et al.*, 1997; *Catuneanu et al.*, 1998], during crustal shortening associated with the subduction and accretion of the paleo-Pacific plate beneath the Gondwana plate [*Hälbich*, 1983, 1993; *Cole*, 1992; *de Wit and Ransome*, 1992]. During the early to mid-Paleozoic, southwestern Gondwana was bordered by a broad, relatively stable continental shelf within a passive margin environment, bordered to the north by Antarctic-like continental ice sheets [*Visser*, 1992]. In the study area, the Karoo Basin starts with glacial sediments in the form of the Dwyka Group (~600–700 m thick) that are abruptly overlain by the postglacial Ecca Group, comprising black shales of the Prince Albert Formation (~150 m) and carbonaceous and pyritic shales of the Whitehill Formation (50–70 m) of the Ecca Group [*Cole*, 1992]. In turn, these are followed by thick massive sandstones and thin shales of the upper Ecca and lower Beaufort Groups [*Cole*, 1992; *Johnson et al.*, 1997]. Overlying this is a 3- to 4-km-thick sequence of terrestrial fluvial deposits, dominated by sandstones and lesser shales (Upper Beaufort), but most of these are not presently exposed in the study area. The total thickness of Karoo Basin ranges from about 5–6 km. Lithologic details are reported by *South African Committee on Stratigraphy* [1980] and *Cloetingh et al.* [1992]. Underlying the Karoo Basin are the siliciclastic rocks of the early Paleozoic Cape Basin, the lowermost sections of which comprise predominantly of thick mature sandstones and quartzites (e.g., Table Mountain sequence). Rocks of the Cape Basin, some 6–10 km in total thickness, are exposed at surface only in the CFB, south of Prince Albert. Drilling shows that some of the Cape Supergroup also underlies the Karoo sediments in the study area but that they thin rapidly northward where they onlap the high-grade Mesoproterozoic basement of the Namaqua-Natal Mobile Belt (NNMB). The precise northern edge of the Cape Basin is not known, but the Cape Supergroup sediment preserved at the northern extremity of the study area are thin to absent. Lithologic details and stratigraphic thicknesses are summarized by *Broquet* [1992].

[10] Drilling has shown that the sediments of the study area unconformably overlie the high-grade gneisses of the NNMB. These gneisses are exposed along the eastern and

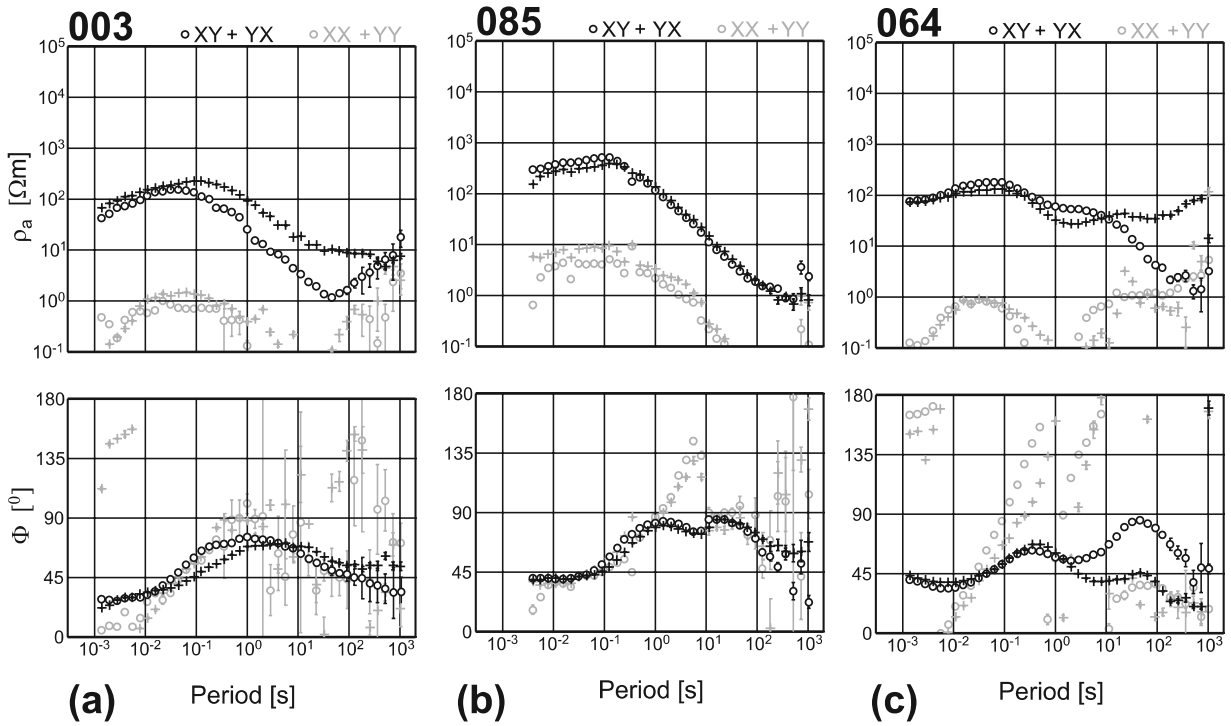

Figure 3. Off-diagonal and diagonal components of (top) apparent resistivity and (bottom) phase of three exemplary sites. (a) Site 003, representative of the area south of the BMA. (b) Site 085, located near the maximum of the BMA. (c) Site 064, situated close to the onset of the Great Escarpment.

western parts of South Africa in the Natal and Namaqualand (Bushmanland and Richtersveld subprovinces), respectively. Both regions were affected by high-grade metamorphism and deformation between 1.0 and 1.1 Ga and on that basis are generally regarded as Grenville-like in age [*Jacobs et al.*, 1993]. However, there are distinct geologic and isotopic (crustal model ages and geochronology) differences between the two regions, and a number of separate terranes have now been identified [*Jacobs et al.*, 1993; *Thomas et al.*, 1994; *Eglington and Armstrong*, 2003]. The Namaqualand metamorphic rocks were derived from older basement, dating between 1.3 and 1.8 Ga and local vestiges of 2.0 Ga. The Natal rocks, on the other hand, comprise of a mosaic of E-W elongated volcanic/plutonic arc terranes dating around 1.1–1.4 Ga [*Thomas et al.*, 1994; *Eglington and Armstrong*, 2003]. The Namaqualand region is also well known for large world class mineral deposits, and the Bushmanland province in particular hosts a number of extensive metamorphosed stratabound massive sulphide ore bodies composed of pyrite, sphalerite and chalcopyrite. In the Natal sector, such extensive mineralization has not been discovered, but prospects of base metal deposits in the southern terranes of Natal, directly along strike with the BMA, are inferred from evidence for exhalative processes and macropyritic lenses in its heterogeneous gneisses and south dipping shear zones [*Thomas et al.*, 1994]. The central portion of the NNMB, as in the present study area, is obscured by the Cape and Karoo basins. Recent isotope analyses on basement rocks recovered from deep drill core (~5.5 km) close to our MT profile (namely, KA/1/66 and QU 1/65, see Figure 2b for location) have greater isotopic similarities to the western Namaqualand sequences and, in particular, the Bushmanland subprovince than those in Natal [*Eglington and Armstrong*, 2003]. Within the Cape Fold Belt, south of the present study area, a number of structural inliers expose older low-grade metasediments intruded by Cambrian granites, all collectively referred to as Saldanian rocks [*Söhnge and Hälbich*, 1983]. The Saldanian rocks are inferred to be part of a more extensive Neoproterozoic (Pan African) basement below the CFB [*Hälbich*, 1993]. If this is correct, then the BMA and the SCCB could also represent a Neoproterozoic suture between the NNMB to the north and the Saldanian province to the south. More recent work, however, shows that the metasediments of these inliers constitute part of the precursor rift sequences of the expansive Cape Basin, and have been deformed and metamorphosed during the CFB orogeny [*Barnett et al.*, 1997]. Thus the NNMB basement may extend below the CFB as far as the southern most continental shelf of Africa [cf. *Hälbich*, 1993]. In summary, there are a number of geologic models that can possibly account for the presence of the BMA and the SCCB, but none of these models are based on robust evidence, for lack of knowledge of the geology below the Karoo Basin and CFB.

3. Magnetotelluric Data Across the BMA

[11] The magnetotelluric (MT) data were collected in March 2004, along a profile between Prince Albert and Fraserburg, crossing the BMA entirely and the northern 100 km of the SCCB (see Figure 2a). GPS synchronized SPAM MkIII [*Ritter et al.*, 1998] and CASTLE broadband instruments together with Metronix MFS05/06 induction coil magnetometers and nonpolarizable Ag/AgCl telluric elec-

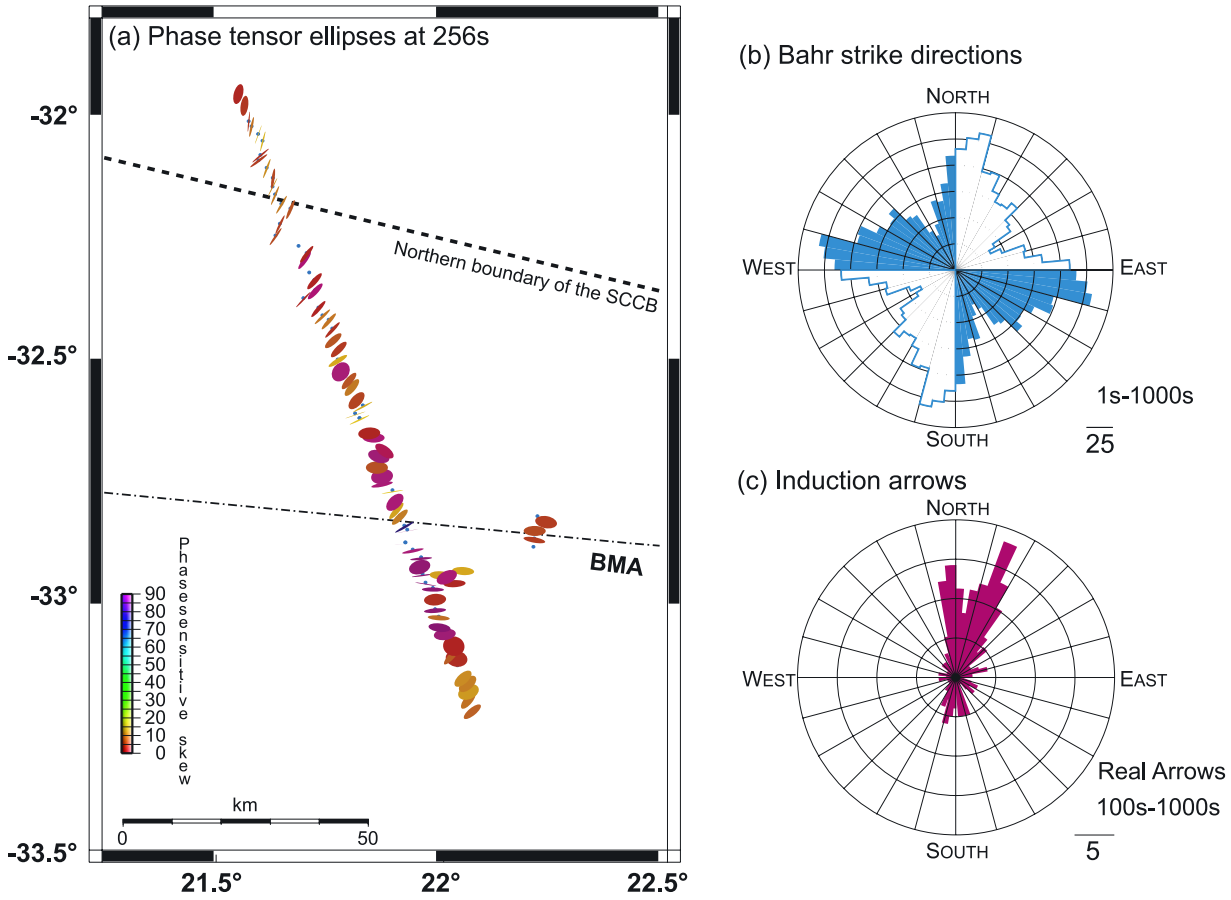

Figure 4. (a) Map of phase tensor ellipses [*Caldwell et al.*, 2004] for a period of 256 s, which is exemplary for a period range from 10 s to 1000 s. In the southern part the ellipses are orientated in E-W direction, whereas in the north we observe a direction of N80°E, which is perpendicular to the MT profile. (BMA, Beattie Magnetic Anomaly; SCCB, Southern Cape Conductive Belt) (b) Regional electric strike angles calculated from the data of all sites in the period range from 1 s to 1000 s using *Bahr*'s [1988] analysis. Open areas represent strike directions with an ambiguity of 90°. (c) Rose diagram for the real induction arrow in the period range from 100 s to 1000 s. The data indicate a predominantly east-west strike direction of the conductivity distribution of the subsurface (geographic coordinate system); however, the accumulation of induction vectors pointing to N20°E is not in perfect agreement with the strike directions obtained from the phase tensor and the phase sensitive approach.

trodes were deployed at 82 sites, giving an average site spacing of 2 km. Five-component electromagnetic field data were recorded in the period range from 0.001 s to 1000 s. The data were processed according to *Ritter et al.* [1998] and *Weckmann et al.* [2005]. Some of the sites were moved to a short parallel profile to avoid noise from a DC railway line. In Figure 3, we show apparent resistivities and phase diagrams, which are derived from the MT impedance tensor. The three sites presented are representative for different areas of this data set. For this diagram, the impedance tensor data are rotated into a geographic coordinate system ($x \hat{=}$ north, $y \hat{=}$ east). The xy and yx component (off-diagonal components) of the apparent resistivity and phase curves of site 003 in Figure 3a vary smoothly and consistently with period. The general trend of the apparent resistivity curves indicates a change from resistive to more conductive to resistive structures with increasing period. The diagonal elements of apparent resistivity and phase (in light grey in Figure 3) are much smaller when compared with the off-diagonal elements. Site 085 (Figure 3b) is located on the roughly E-W striking maximum of the magnetic anomaly. Here, both off-diagonal components show steeply decreasing apparent resistivity curves from approximately 500 Ω m at 0.1 s to 1 Ω m at 1000 s and a consistent increase in the phase values. Site 064, on the other hand, which is located close to the Great Escarpment, indicates apparent resistivity curves with a more complex succession of conductive and resistive parts (Figure 3c). This feature in the apparent resistivity curves is visible at many sites of the northern third of the profile.

[12] Working along profiles implies that the region is dominated by a two-dimensional distribution of the electrical conductivity. In order to determine a geoelectric strike direction and the dimensionality of the subsurface from the MT data, tensor decomposition schemes [*Bahr*, 1988; *Smith*, 1995] are applied. Figure 4 shows a map of the phase tensor ellipses [*Caldwell et al.*, 2004] for a period of 256 s and strike angles obtained from *Bahr*'s [1988] phase-sensitive approach

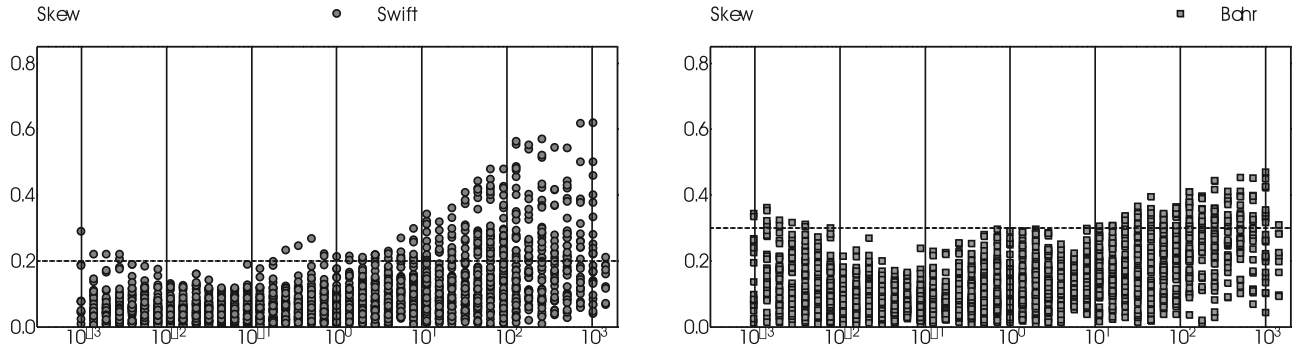

Figure 5. (left) *Swift* [1967] and (right) *Bahr* [1988] skew values for all sites. We observe skew values over the empirical threshold of 0.2 (Swift) and 0.3 (Bahr) only at long periods.

in combination with the directions of the induction vectors in form of rose diagrams in a geographic coordinate system. The phase tensor ellipses map lateral conductivity variations with the orientation of their major axes. They are either orientated parallel or perpendicular to a conductivity contrast depending whether a particular site is located on the conductive or resistive side of the contrast. Along our profile we can observe a change from predominantly E-W orientated ellipses in the south to more SW-NE orientated ellipses in the north. A similar situation is expressed in the phase sensitive strike directions which are presented as a cumulative value for all sites in the period range from 1 s to 100 s in Figure 4b. The preferred strike direction is approximately N100°E with a deviation of ±15°. A general E-W strike is also in agreement with the regional strike of the tectonic features [*Söhnge and Hälbich*, 1983; *Harvey et al.*, 2001]. The induction vectors, which are oriented perpendicular to a close-by lateral conductivity contrast, support an E-W strike direction. However, we observe two maxima of the induction vectors: (1) in north direction and (2) in N20°E. The latter strike direction is not in perfect agreement with the electrical strike directions obtained from the phase tensor and the phase sensitive approach but might reflect deviation from the pure two-dimensional (2-D) setting. Finally, we rotated the MT impedance tensor into the geographic east direction and projected the MT sites onto a N-S orientated profile (see grey dot-dashed line in Figure 2b). This implies that for further 2-D modeling the xy component of the MT impedance tensor represents the E polarization data with electric currents flowing along strike and the yx component represents the B polarization with current systems perpendicular.

[13] Usually, the skewness of the MT impedance tensor is evaluated to estimate the dimensionality of the data. The diagram shows *Swift* [1967] (Figure 5, left) and phase sensitive *Bahr* [1988] (Figure 5, right) skew values for all sites in a period range from 0.001 s to 1000 s; the (dashed)

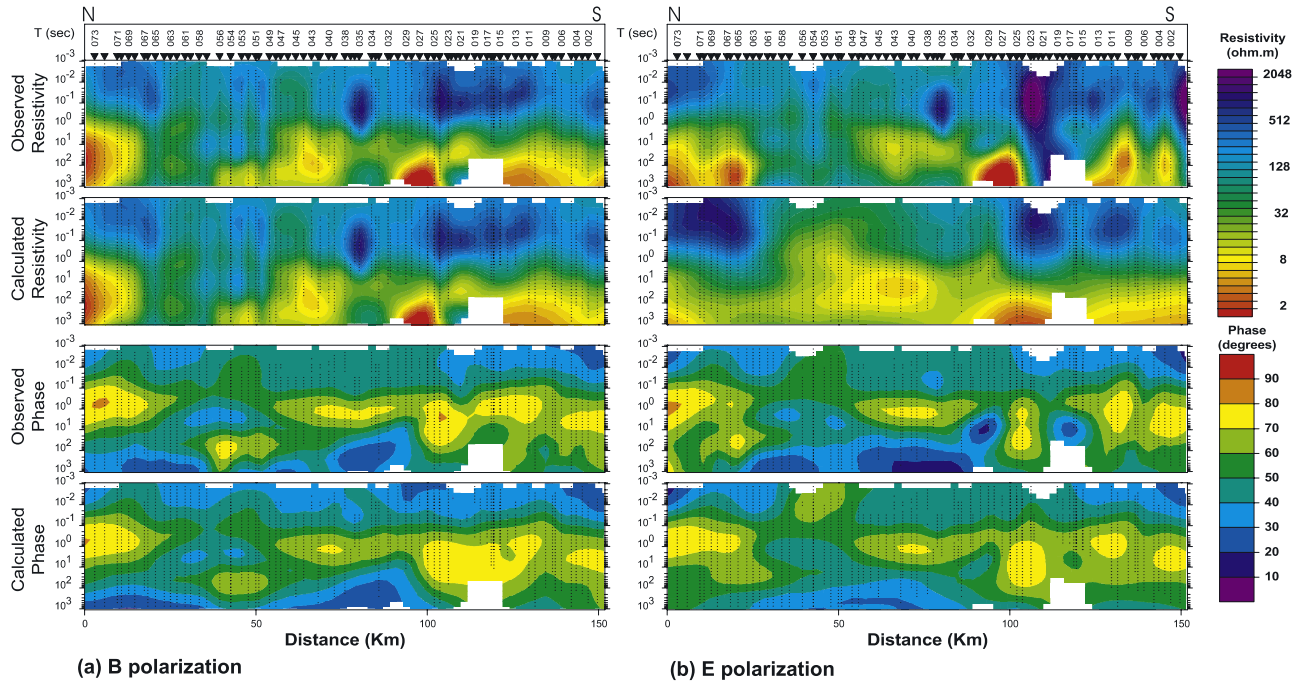

Figure 6. Data and model responses of the (a) B and (b) E polarization in form of a pseudosection plot along the entire profile. The vertical axis represents the period axis [s]. (top) Apparent resistivities and (bottom) phases.

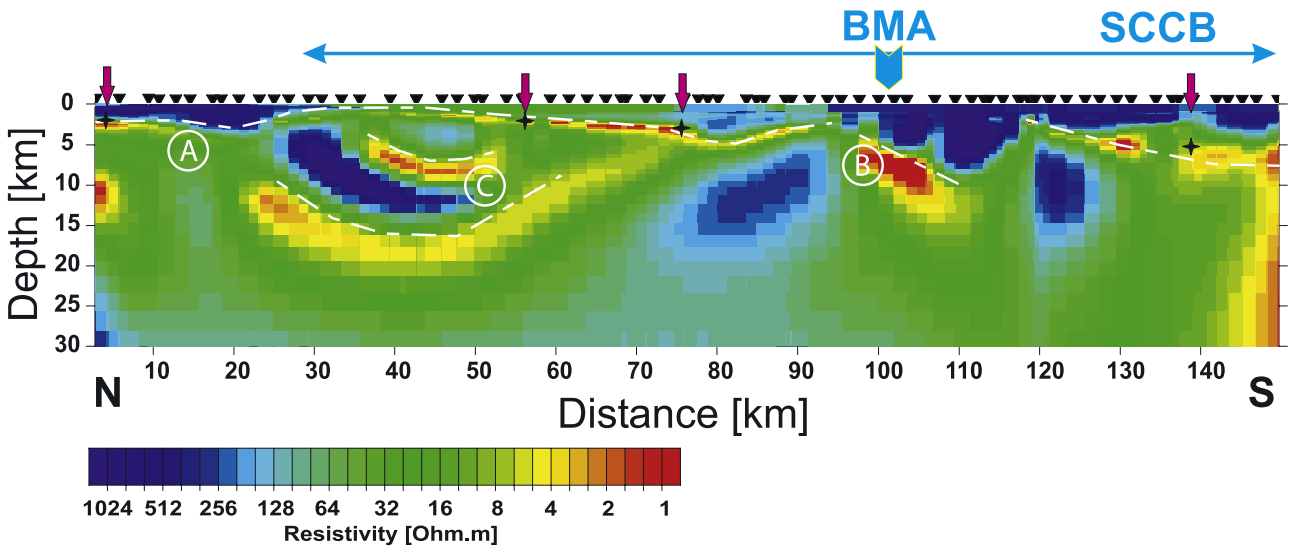

Figure 7. Conductivity model obtained from the 2-D inversion algorithm by *Rodi and Mackie* [2001]. Site locations are indicated by black triangles. The axis of the BMA and the extent of the SCCB are indicated by arrows. The data reveal several previously unknown conductive structures (red and yellow). The most prominent conductivity anomaly (B) is located beneath the surface trace of the BMA. Two conductive structures located above and below a resistive layer (C) may define a large synform, ~50 km across, within the NNMB. A shallow subhorizontal band of high conductivity (A) can be observed in the upper 5 km, deepening toward the southern part of the section, near Prince Albert, where the Karoo basin is known to be thickest [*Cole*, 1992]. Red arrows at the surface indicate the location of deep boreholes which were projected onto the profile. The black crosses indicate the depth in which the carbonaceous and pyritiferous black shales of the Whitehill Formation were found in the borehole.

lines indicate empirically determined thresholds of 0.2 (Swift) and 0.3 (Bahr) above which a 2-D assumption cannot be maintained [*Bahr*, 1991]. There are some skew values above 0.2 for the Swift skew; however, most of the phase sensitive skew values are below 0.3.

[14] The MT data, separated into E and B polarization, are shown as pseudosections of apparent resistivity and phase in Figure 6 together with the calculated results of the 2-D inversion image (see Figure 7). Both polarizations give a similar apparent resistivity pattern and especially for the short periods we observe similar values of the apparent resistivities, which indicate that static shift is only a minor problem. Comparing the period range from 0.001 s to 1 s three major zones can be distinguished: In the southern part up to site 040 we observe relatively resistive structures, in the middle part of the profile (sites 041 to 063) electrical resistivities are lower by an order of magnitude to rise again on the high plateau north of the Great Escarpment. The long-period parts of the pseudosections are generally more conductive (30–2 Ω m); additionally, we can identify some zones of high electrical conductivities: The northern 10 sites exhibit apparent resistivities of 2 Ω m between periods of 1 s and 1000 s farther to the south with its maximum beneath site 043, where we observe apparent resistivities of around 8 Ω m. In the southern half of the pseudosections beneath sites 030–024 and the southern most 15 sites show high conductivity at long periods.

4. The 2-D Inversion

[15] The resistivity section in Figure 7 is the result of a 2-D inversion using the RLM2DI algorithm after *Rodi and Mackie* [2001] which is part of the WinGLink (available at http://www.geosystem.net/software.htm) software package. This inversion scheme finds regularized solutions to the two-dimensional inverse problem for MT data using the method of nonlinear conjugate gradients. For the inversion we used a grid of 207 cell horizontally and 158 cells vertically. This high number of grid cells, especially in the vertical direction, was necessary as topography was included and to keep cells approximately in square shape for the shallow subsurface. Both the E and B polarization data were jointly inverted with an intermediate inclusion of the vertical magnetic field data. Thereby the code iterated for approximately 200 times using only the MT impedance tensor data; afterward, we inverted for E and B polarization together with the vertical magnetic field for another 50 iterations. In a final step, in which we also reached convergence, we inverted again only the MT data for approximately 50–100 iterations. By using the statistically derived data errors for the inversion the short-period data are favored over long-period data, because the number of estimates decreases rapidly with increasing period which is expressed in larger error bars. Instead of using the experimental data errors we therefore preset error bounds of 5% for B polarization apparent resistivity, 100% for E polarization apparent resistivity and 0.6° for E and B polarization phases. The high error bounds set for the E polarization apparent resistivity reduces the influence of static shift effects as the emphasis on fitting the data is on the phases. The inversion algorithm searches for a minimum structure model with the lowest overall misfit. The trade-off between data misfits and model smoothness is controlled by the

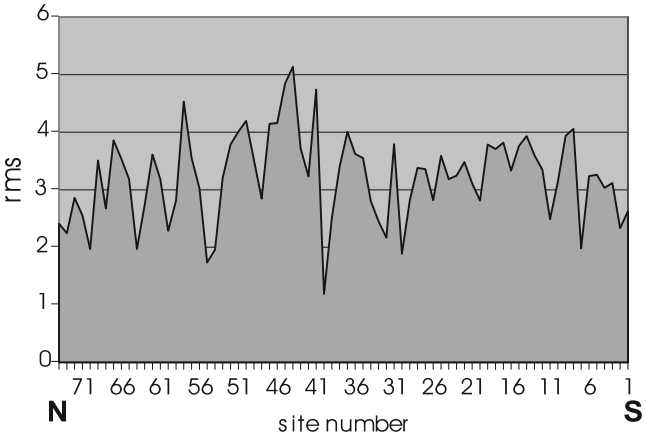

Figure 8. RMS error versus site number showing that there is no systematic misfit of a subset of data or certain areas of the model.

regularization parameter τ. This parameter is not determined automatically, but found through several runs of the inversion using different values. In our case, a setting of τ = 15 seems to be a good compromise between model roughness and data misfit. For the section presented we started the inversion from a homogeneous half space model of 100 Ω m. However, different starting models, e.g., with different conductivities were tested to asses the influence of the starting model on the resulting model. A statistical analysis of the cell conductivities in the inner part of the model after conversion of the inversion shows independence of the starting model value of 100 Ω m.

[16] The 2-D inversion model reveals several high-conductivity structures within the SCCB and the Karoo Basin (shown in red and yellow in Figure 7). The most striking one is probably the anomaly which seems to be spatially coincident with the surface trace of the BMA (labeled B in Figure 7). This conductivity anomaly is inclined toward the south and located in 5 km depth reaching down to approximately 12 km depth. Additionally, two deep reaching (8–20 km) features (C) can be found farther to the north located at the northern boundary of the SCCB which also coincides with the onset of the Great Escarpment. They are synformal in shape and have resistivity values of 1 Ω m. In the upper 5 km we observe a subhorizontal band of high conductivity (A). Additionally, we observe a generally high conductive crust (20–60 Ω m), whereas below 45 km depth and the area north of the profile are much more resistive (>500 Ω m). The conductive feature at the southern edge of the profile is most likely an artefact from the inversion. It is possible, however, that the long-period data of the southern most sites begin to sense the highly conductive Kango and Oudtshoorn basins, approximately 40 km to the south of our profile.

[17] The overall normalized RMS misfit of the final model is 3.2%. The misfit is dominated by a poorer fit of the E polarization data at longer periods as a comparison of observed and calculated apparent resistivities and phases in Figure 6 exhibits. The RMS errors of each site in Figure 8 show that there is no systematic misfit of a subset of data or certain areas of the model. In order to assess the robustness of the conductive features and to test the choice of geoelectrical strike, we also computed models in a coordinate system following the profile, with B polarization parallel to the profile and E polarization perpendicular. The obtained electrical conductivity image (not shown) is generally similar to the one in Figure 7; however, anomaly B beneath the axis of the BMA is bend a bit more into the horizontal line in 12 km depth and two synformal structures C seem to merged at their southern extremity. The location and shape of the subhorizontal conductivity band A remains the same.

5. Interpretation and Discussion

[18] The MT method is more sensitive to conductive constituents in pore volumes than to the rock matrix itself. Even small amounts of fluids, melt, ores, graphite, sulfide etc. can lower the bulk resistivity of rocks significantly if they form interconnected networks [*Jödicke et al.*, 2004; *Brown*, 1994]. Thus interpreting zones of high conductivity often requires additional information from other disciplines or boreholes.

[19] For the shallow conductivity anomalies, additional information could be obtained from deep boreholes. In the Karoo Basin a number of deep boreholes up to 5.5 km in depth were drilled during exploration for coal, oil, and uranium [*Leith*, 1969; *Eglington and Armstrong*, 2003]. The data are available on open file (National Core Library, 2005, http://196.33.85.14/cgs_inter/content/view/236/296/). We use stratigraphic information from four boreholes, projected into our section line, to constrain the nature of the shallow conductivity anomalies, that we have identified in the upper 5 km of our section (Figure 2b). All four boreholes intersect black carbonaceous shales of the Whitehill Formation, at depths varying between 2 and 5 km in the region adjacent to our survey line. The Whitehill Formation in this region varies in thickness between 50 and 70 m of black pyritic shales with up to 14 wt % carbonaceous matter [*Rogers*, 1925]. The Whitehill Formation is regionally very persistent in thickness and composition, and can be traced throughout the entire Karoo Basin and its equivalents in the Paraná Basin of South America, where it is known as the Irati Formation [*Du Toit*, 1927; *South African Committee on Stratigraphy*, 1980; *Milani*, 1992; *le Roux*, 1995]. The correlation of the high-conductivity band and Whitehill Formation in our study area unquestionably reveals that black carbonaceous shales in the Karoo Basin are the cause of the shallow and subhorizontal high-conductivity anomaly. In turn this allows us to interpret the offset of this anomaly just north of Prince Albert as a ''blind'' south dipping thrust or overturned synform.

[20] The interpretation of the deeper anomalies is more difficult as geological constraints are missing. The northern conductors as well as the conductor beneath the surface trace of the BMA are located at midcrustal levels of the NNMB and are likely Mesoproterozoic structures. Existing tectonic reconstructions and geological sections of the NNMB and the CFB included the BMA as a 20 km broad and 30 km deep reaching tectonic sliver of serpentinized oceanic crust [*Pitts et al.*, 1992]. However, such a feature is incompatible with our conductivity image. Serpentinite in general is only conductive in active regimes when fluids are released during its formation and thereby lower the resistivity [*Bruhn et al.*, 2001]; in fossil regimes, free fluids are

not likely retained at midcrustal depths. Alternatively serpentinite generally contain amounts of disseminated magnetite, exolved from olivine during serpentinization. The presence of metamorphic magnetite could explain the magnetic anomalies, but for a large conductivity anomaly, magnetite would be required to be interconnected over substantial distances. However, because the MT method is not sensitive to magnetic anomalies, it cannot be concluded that the conductivity anomaly beneath the trace of the BMA is also the source of the magnetic anomaly. We believe, it is much more consistent with other findings in similar settings to attribute the high conductivities to crustal-scale shear zones. Fossil shear zones become visible with MT in presence of graphite enrichment on shear planes as observed in the Damara Belt in Namibia [*Ritter et al.*, 2003; *Weckmann et al.*, 2003]. In the Natal sector of the NNMB, major shear zones separate at least 4 tectonic terranes of different crustal characters. Magnetic anomalies with similar characteristics to the Beattie anomaly flank the shear zones that constitute the terrane boundaries, including the extension of the Beattie anomaly to the Natal coast [*Thomas et al.*, 1992]. Therefore concave-shaped conductivity anomalies at the northern boundary of the SCCB might be related to folded subhorizontal thrust or shear zones within the Natal sector of the Mesoproterozoic NNMB [*Eglington and Armstrong*, 2003]. It is also conceivable, however, that the observed anomalies image mineralized synforms. Farther to the NW within the Bushmanland subprovince of the Namaqualand, large world class stratabound ore bodies are hosted in intensely deformed gneisses that have been refolded into late open synforms [*Ryan et al.*, 1986]. In this context, the high conductivities might image mineralized tectonic synforms within the NNMB rather than a wedge of serpentinized oceanic crust. Further work is needed to test this interpretation.

[21] In conclusion, our new high-resolution MT results have identified a regional shallow and relatively thin subhorizontal anomaly that can be linked to an extensive stratigraphic horizon near the base of the Karoo Basin. Our data, furthermore, support the existence of a deeper conductivity belt, but allow for a much better definition of crustal conductivity in this region because of the dense site spacing. Such laterally confined zones of crustal conductivity could not be resolved with the magnetometer array study by *de Beer and Gough* [1980] with a station separation in the order of 100–150 km and recordings only at long periods (1000–30000 s).

[22] **Acknowledgments.** Field work in South Africa was funded by the GeoForschungsZentrum Potsdam. We thank the Geophysical Instrument Pool Potsdam for providing the MT equipment. This experiment would not have been possible without the dedicated field and logistic support of Rod Green and the generous permission of the local farmers for access to their land. We also appreciate the help of Juliane Hübert, Ulrich Kniess, Tshifi Mabidi, and Jacek Stankiewicz during our fieldwork. U.W. was supported by the Emmy Noether fellowship of the German Science Foundation DFG. We would like to thank two anonymous reviewers and particularly Ulrich Schmucker for their comments. This is an Inkaba yeAfrica contribution 02.

References

Bahr, K. (1988), Interpretation of the magnetotelluric impedance tensor: Regional induction and local telluric distortion, *J. Geophys.*, *62*, 119–127.

Bahr, K. (1991), Geological noise in magnetotelluric data: A classification of distortion types, *Phys. Earth Planet. Inter.*, *66*, 24–38.

Barnett, W., R. Armstrong, and M. de Wit (1997), Stratigraphy of the upper Neoproterozoic Kango and lower Paleozoic Table Mountain Group of the Cape Fold Belt revisited, *S. Afr. J. Geol.*, *100*(3), 237–250.

Beattie, J. (1909), *Report of the Magnetic Survey of South Africa*, Cambridge Univ. Press, New York.

Bochannon, J. (2004), Earth Sciences seek niche apart form mining industry, *Science*, *304*, 380–381.

Broquet, C. (1992), The sedimentary record of the Cape Supergroup: A review, in *Inversion Tectonics of the Cape Fold Belt, Karoo and Cretaceous Basins of Southern Africa*, edited by M. de Wit and I. Ransome, pp. 159–183, A. A. Balkema, Brookfield, Vt.

Brown, C. (1994), Tectonic interpretation of regional conductivity anomalies, *Surv. Geophys.*, *15*(1), 123–158.

Bruhn, D., F. Schilling, S. Raab, E. Spangenberg, and B. Wunder (2001), Physical properties of dehydrating serpentinite, *Eos Trans. AGU*, *82*(47), Fall Meet. Suppl., Abstract T31B–0845.

Caldwell, T. G., H. M. Bibby, and C. Brown (2004), The magnetotelluric phase tensor, *Geophys. J. Int.*, *158*(2), 457–469, doi:10.1111/j.1365-246X.2004.02,281.x.

Catuneanu, O., P. Hancox, and B. Rubidge (1998), Reciprocal flexural behaviour and contrasting stratigraphies: A new basin development model for the Karoo retroarc foreland system, South Africa, *Basin Res.*, *10*, 417–439.

Cloetingh, S., A. Lankreijer, M. de Wit, and H. Martinez (1992), Subsidence history analysis and forward modeling of the Cape and Karoo Supergroups, in *Inversion Tectonics of the Cape Fold Belt, Karoo and Cretaceous Basins of Southern Africa*, edited by M. de Wit and I. Ransome, pp. 239–249, A. A. Balkema, Brookfield, Vt.

Cole, D. (1992), Evolution and development of the Karoo Basin, in *Inversion Tectonics of the Cape Fold Belt, Karoo and Cretaceous Basins of Southern Africa*, edited by M. de Wit and I. Ransome, pp. 87–99, A. A. Balkema, Brookfield, Vt.

Corner, B. (1989), The Beattie anomaly and its significance for crustal evolution within the Gondwana framework, paper presented at First Technical Meeting, S. Afr. Geophys. Assoc., Johnannesburg.

de Beer, J., and D. Gough (1980), Conductive structures in southernmost Africa: A magnetometer array study, *Geophys. J. R. Astron. Soc.*, *63*, 479–495.

de Beer, J., J. van Zijl, and D. Gough (1982), The Southern Cape Conductive Belt (South Africa): Its composition, origin and tectonic significance, *Tectonophysics*, *83*, 205–225.

de Wit, M., and B. Horsfield (2006), Inkaba yeAfrica project surveys sector of Earth from core to space, *Eos Trans. AGU*, *87*(11), 113.

de Wit, M., and I. Ransome (Eds.) (1992), *Inversion Tectonics of the Cape Fold Belt, Karoo and Cretaceous Basins of Southern Africa.*, A. A. Balkema, Brookfield, Vt.

Du Toit, A. (1927), *A Geological Comparison of South America With South Africa*, 158 pp., Carnegie Inst. of Washington, Washington, D. C.

Eglington, B., and R. Armstrong (2003), Geochronological and isotopic constraints on the Mesoproterozoic Namaqua-Natal Belt: Evidence from deep borehole intersections in South Africa, *Precambrian Res.*, *125*, 179–189.

Gough, D., J. de Beer, and J. van Zijl (1973), A magnetometer array study in southern Africa, *Geophys. J. R. Astron. Soc.*, *34*, 421–433.

Hälbich, I. (1983), A geodynamic model for the Cape Fold Belt, in *Geodynamics of the Cape Fold Belt*, edited by A. Söhnge and I. W. Hälbich, *Spec. Publ. Geol. Soc. S. Afr., 12*, 177–184.

Hälbich, I. (1993), Cape Fold Belt–Agulhas Bank Transect across Gondwana suture, southern Africa, *Geosci. Transect*, vol. 9, 18 pp., AGU, Washington, D. C.

Harvey, J., M. de Wit, J. Stankiewicz, and C. Doucoure (2001), Structural variations of the crust in the southwest Cape, deduced from seismic receiver functions, *S. Afr. J. Geol.*, *104*, 231–242.

Jacobs, J., R. Thomas, and K. Weber (1993), Accretion and indentation tectonics at the southern margin of the Kaapvaal craton during the Kibaran (Grenville) orogeny, *Geology*, *21*, 203–206.

Jödicke, H., J. H. Kruhl, C. Ballhaus, P. Giese, and J. Untiedt (2004), Syngenetic, thin graphite-rich horizons in lower crustal rocks from the Serre San Bruno, Calabria (Italy), and implications for the nature of high-conducting deep crustal layers, *Phys. Earth Planet. Inter.*, *141*, 37–58.

Johnson, M., C. van Vuuren, J. Visser, D. Cole, H. de Wickens, A. Christie, and D. Roberts (1997), The Foreland Karoo Basin, South Africa, in *Sedimentary Basins of the World*, vol. 3, *African Basins*, edited by R. Selley, pp. 269–317, Elsevier, New York.

King, L. (1963), *South African Scenery*, 308 pp., 3rd ed. Oliver and Boyd, London.

Leith, M. J. (1969), Internal well completion report, technical report, Counc. for Geosci., Pretoria.

le Roux, J. (1995), Heartbeat of a mountain: Diagnosing the age of depositional events in the Karoo (Gondwana) Basin from the pulse of the Cape Orogen, *Geol. Rundsch.*, *84*, 626–635.

Milani, E. (1992), Intraplate tectonics and the evolution of the Parana basin, SE Brasil, in *Inversion Tectonics of the Cape Fold Belt, Karoo and Cretaceous Basins of Southern Africa*, edited by M. de Wit and I. Ransome, pp. 101–115, A. A. Balkema, Brookfield, Vt.

Pitts, B., M. Mahler, J. de Beer, and D. Gough (1992), Interpretation of magnetic, gravity and magnetotelluric data across the Cape Fold Belt and Karoo Basin, in *Inversion Tectonics of the Cape Fold Belt, Karoo and Cretaceous Basins of Southern Africa*, edited by M. de Wit and I. Ransome, pp. 27–32, A. A. Balkema, Brookfield, Vt.

Ritter, O., A. Junge, and G. J. Dawes (1998), New equipment and processing for magnetotelluric remote reference observations, *Geophys. J. Int.*, *132*, 535–548.

Ritter, O., U. Weckmann, T. Vietor, and V. Haak (2003), A magnetotelluric study of the Damara Belt in Namibia 1. regional scale conductivity anomalies, *Phys. Earth Planet. Inter.*, *138*, 71–90, doi:10.1016/S0031-9201(03)00,078-5.

Rodi, W., and R. L. Mackie (2001), Nonlinear conjugate gradients algorithm for 2D magnetotelluric inversion, *Geophysics*, *66*, 174–187.

Rogers, A. (1925), The geology of the country around Laingsburg, technical report, Geol. Surv. of the Union of S. Afr., Pretoria.

Ryan, P., A. Lawrence, R. Lipson, J. Moore, A. Paterson, D. Stedman, and D. van Zyl (1986), The Aggeneys base metal sulphide deposits, Namaqualand District, in *Mineral Deposits of Southern Africa*, edited by C. R. Annhaeusser and S. Maske, pp. 1447–1473, Geol. Soc. South Afr., Johannesburg.

Smith, J. T. (1995), Understanding telluric distortion matrices, *Geophys. J. Int.*, *122*, 219–226.

Söhnge, A., and I. W. Hälbich (Eds.) (1983), *Geodynamics of the Cape Fold Belt*, *Spec. Publ. Geol. Soc. S. Afr.*, *12*.

South African Committee on Stratigraphy (1980), Stratigraphy of South Africa, Handbook 8,technical report, Geol. Surv. of S. Afr., Pretoria.

Swift, C. (1967), *A magnetotelluric investigation of an electrical conductivity anomaly in the southwestern United States*, Ph.D. thesis, Mass. Inst. of Technol., Cambridge.

Thomas, R., C. Marshal, Du A. Plessis, F. Fitch, J. Miller, von V. Brunn, and M. Watkeys (1992), Geological studies in southern Natal and Transkei: Implications for the Cape Orogen, in *Inversion tectonics of the Cape Fold Belt, Karoo and Cretaceous Basins of Southern Africa*, edited by M. de Wit and I. Ransome, pp. 229–236, A. A. Balkema, Brookfield, Vt.

Thomas, R., A. Agenbacht, D. Cornel, and J. Moore (1994), The Kibaran of southern Africa: Tectonic evolution and metallogeny, *Ore Geol. Rev.*, *9*, 131–160.

Visser, N. J. N. (1992), Deposition of the Early to Late Permian Whitehill Formation during a sea-level highstand in a juvenile foreland basin, *S. Afr. J. Geol.*, *95*(5-6), 109–115.

Weckmann, U., O. Ritter, and V. Haak (2003), A magnetotelluric study of the Damara Belt in Namibia—2. MT phases over 90° reveal the internal structure of the Waterberg Fault/Omaruru Lineament, *Phys. Earth Planet. Inter.*, *138*(2), 91–112, doi:10.1016/S0031-9201 (03)00079-7.

Weckmann, U., A. Magunia, and O. Ritter (2005), Effective noise separation for magnetotelluric single site data processing using a frequency domain selection scheme, *Geophys. J. Int.*, *161*(3), 635–652, doi:10.1111/j.1365-246X.2005.02,621.x.

T. Branch and M. de Wit, CIGCES, Department of Geological Sciences, University of Cape Town, Rondebosch, 7700, Republic of South Africa.

A. Jung, O. Ritter, and U. Weckmann, GeoForschungsZentrum Potsdam, Telegrafenberg, D-14473 Potsdam, Germany. (uweck@gfz-potsdam.de)